SCIENTIFIC REPORTS

OPEN

Different Synchrony in Rhythmic Movement Caused by Morphological Difference between Five- and Six-armed Brittle Stars

Received: 11 October 2018
Accepted: 24 May 2019
Published online: 05 June 2019

Daiki Wakita[1], Yumino Hayase[2] & Hitoshi Aonuma[1,3]

Physiological experiments and mathematical models have supported that neuronal activity is crucial for coordinating rhythmic movements in animals. On the other hand, robotics studies have suggested the importance of physical properties made by body structure, i.e. morphology. However, it remains unclear how morphology affects movement coordination in animals, independent of neuronal activity. To begin to understand this issue, our study reports a rhythmic movement in the green brittle star *Ophiarachna incrassata*. We found this animal moved five radially symmetric parts in a well-ordered unsynchronized pattern. We built a phenomenological model where internal fluid flows between the five body parts to explain the coordinated pattern without considering neuronal activity. Changing the number of the body parts from five to six, we simulated a synchronized pattern, which was demonstrated also by an individual with six symmetric parts. Our model suggests a different number in morphology makes a different fluid flow, leading to a different synchronization pattern in the animal.

Animals exhibit a variety of rhythmic movements, such as locomotion, mastication and ventilation. It is generally accepted that animals utilize neuronal activity to coordinate the movements of distant body parts, such as left and right limbs in walking. Many studies have demonstrated the relationship between neuronal interactions and movement coordination by mathematical models. One such successful model to explain the swimming patterns of lampreys was built based on the results of physiological experiments and simulated swimming movements[1]. A genetics study using transgenic mice experimentally changed the coordinated patterns of left and right limbs to reveal the role of specific neurons in locomotion[2]. On the other hand, robotics studies have suggested the importance of physical properties in body for such coordination. For example, four-limbed robots demonstrated different locomotion patterns depending on the loading weight or the swing speed of each motor-driven limb although the limbs were physically connected without electrical circuitry (i.e. neuronal circuitry in animals)[3,4]. A brittle-star-like robot designed by a similar concept was able to immediately change locomotion patterns owing to the unexpected loss of limbs[5]. In these robots, the coordinated patterns of body parts are directly influenced by body structure, i.e. morphology. Supposedly, such a morphological role independent of electricity is also utilized in animals as non-neuronal interactions. However, it remains an issue of how morphology affects such coordinated movements in animals. This problem arises from the lack of examples in which obviously different morphology results in obviously different coordinated patterns in animals.

To break this impasse, we here report a rhythmic movement in the green brittle star *Ophiarachna incrassata* (Lamarck, 1816). This marine animal is characterized by radial symmetry in morphology, as recognized in other echinoderms. The central disk has typically five arms, which partition the disk into five symmetric fan-shaped parts, called interradii. Our subject is its movement which comprises several cycles of shrinkage and expansion in the five interradii and frequently occurs after feeding (Fig. 1, Supplementary Video S1). Individuals that were kept without feeding even for a week never showed the movement, implying a relationship with digestion. We termed this rhythmic movement "*pumping*" because it was reminiscent of pumps. The movements between the five interradii were regularly ordered without synchronization. Based on our mathematical model, this coordinated pattern

[1]Graduate School of Life Science, Hokkaido University, Sapporo, 060-0810, Japan. [2]Graduate School of Science, Hiroshima University, Higashi-Hiroshima, 739-8526, Japan. [3]Research Institute for Electronic Science, Hokkaido University, Sapporo, 060-0812, Japan. Correspondence and requests for materials should be addressed to H.A. (email: aon@es.hokudai.ac.jp)

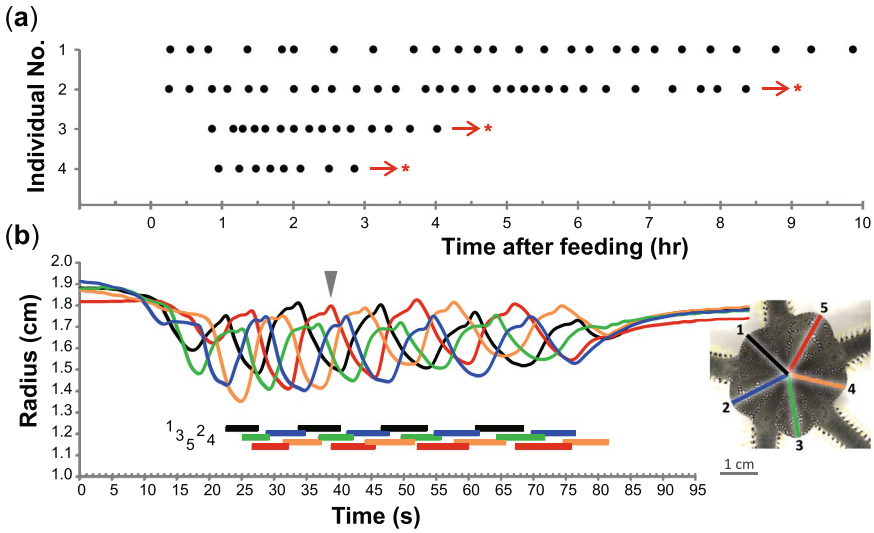

Figure 1. Rhythmic movement, "pumping", in the five-armed individuals of the green brittle star *Ophiarachna incrassata*. (**a**) Temporal frequency of pumping phases. Each point represents a pumping phase, which comprises a series of movements shown in (**b**). The animals exhibit the first pumping phase 36 ± 17 min (N = 4) after feeding. Then, they periodically initiate pumping for more than 10 hrs. The interval between pumping phases is not consistent (20 ± 9 min) among individuals. Asterisks indicate no record from the arrows. (**b**) Temporal change in the radius of the five interradii in a pumping phase. Inset shows the aboral side of an individual at the moment indicated by the arrowhead in the graph. Radius is measured from the center of the disk to the midpoint of the edge of each interradius. The radii numbered anticlockwise are colored as in the inset, which corresponds to the graph in color. Colored horizontal bars under the graph represent shrinking periods of each interradius.

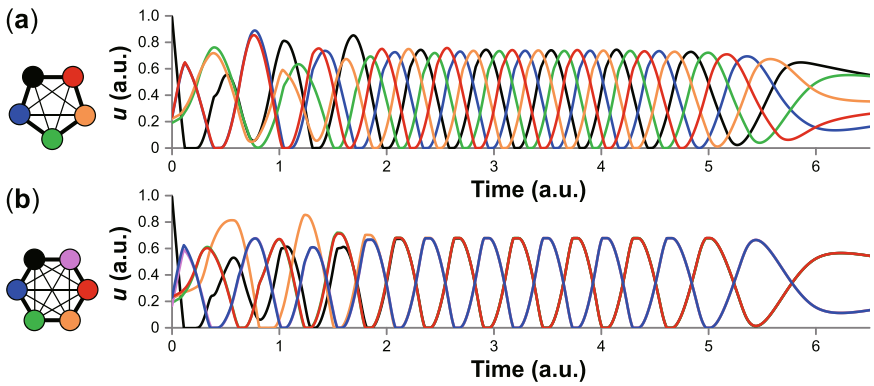

Figure 2. Simulation of rhythmic movement, "pumping", in the green brittle star *Ophiarachna incrassata*, based on a phenomenological model. (**a**) Temporal change of the volume of five interradii. Cycles are unsynchronized as in the experiments of five-armed individuals (see Fig. 1b). (**b**) Temporal change of the volume of six interradii. Three distant interradii and the other three each make synchronized groups, anticipating the coordinated pattern of six-armed individuals. *u* in the y-axis represents the volume of internal fluid in the interradii. Each axis is given in an arbitrary unit. The color of the interradii in each inset corresponds to that of each graph. The black one in each panel represents the 1st interradius, which initially has a larger volume than the others.

can be easily explained by physical properties without considering neuronal interactions. We then changed the number of interradii in the model, referring to the fact that brittle stars sometimes have individual difference in the number of arms, namely, the number of interradii. Simulation after changing from five to six interradii made synchronized movements between the interradii (Fig. 2). We finally obtained a six-armed individual, which demonstrated the synchronized movements (Fig. 3, Supplementary Video S2). Therefore, pumping will provide a model system to understand the role of morphology in movement coordination utilized in actual animals.

Results

Behavior in five-armed brittle stars. The rhythmic movement in the five-armed individuals of the green brittle star, pumping, was frequently observed with an interval of 21 ± 10 min (mean ± s.d., N = 4) after feeding (Fig. 1a). Each continuously moving phase, termed "*pumping phase*", started with a closing of the mouth and

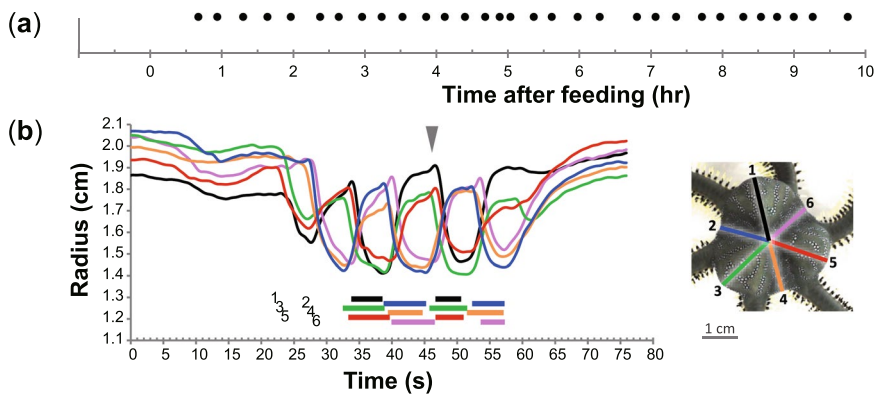

Figure 3. Rhythmic movement, "pumping", in the six-armed individual of the green brittle star *Ophiarachna incrassata*. (**a**) Temporal frequency of pumping phases. The animal frequently shows pumping phases for more than 10 hrs after feeding, as occurs in five-armed animals. (**b**) Temporal change in the radius of the six interradii in a pumping phase. Cycles are synchronized with two groups separated, which demonstrates the model simulation of six interradii (see Fig. 2b). Figures are shown as in Fig. 1.

genital slits on the oral side of the disk. The whole contraction of the disk was immediately followed by a series of shrinkage and expansion in interradii. Five-armed individuals produced a pumping phase for 57 ± 12 s (N = 2, n = 6), in which each of the five interradii repeated 3–5 cycles of the movements. Based on the radius of the interradii in the aboral view, each cycle comprised a shrinking period for 5.9 ± 1.0 s and an expanding period for 6.5 ± 0.8 s at the beginning of the pumping phase (Fig. 1b). These phases gradually became longer to 7.6 ± 1.0 and 8.1 ± 0.9 s respectively at the end. Meanwhile, the amplitude of the movements gradually became smaller. Each expanding period included two increasing stages in radius; the first longer one was recognized as an increase in the volume of the interradii, while the second shorter one was apparently ascribed to change in the form of the interradii. Numbered from 1 to 5 anticlockwise in the aboral view, the interradii regularly moved in the unsynchronized sequence of 1-3-5-2-4 or 1-4-2-5-3 repetitively; a cycle in one of the five interradii was followed by that in either of two distant ones with 2.2 ± 0.5 s delayed (Fig. 1b, Supplementary Video S1). The two types of sequence were observed in the same individual although a continuous pumping phase underwent either one consistently. The initially shrinking interradius was not always identical. At the end of the pumping phase, the mouth and genital slits slowly opened, so that the disk became relaxed as usual.

Modelling and simulation. To explain the relationship between the pumping pattern and morphology, we used a mathematical model. Previous models explained how differences in network structure caused difference in rhythmic outputs on the basis of neuronal networks where a certain number of neurons constituted a ring[6–8]. These models were inspired in contexts irrelevant to pumping; nevertheless, they demonstrated that a pumping-like rhythmic pattern was generated among five neurons which laterally inhibited each other. Although brittle stars possess a nerve ring in the disk[9], it is unclear whether they utilize such a neuronal network. We suppose that their simple nervous system is insufficient to coordinate the dynamic movements of pumping, and rather physical properties of their body have a dominant effect. We thus constructed a phenomenological model simply focusing on the external morphological change in interradii, independent of neuronal interactions.

We assumed that internal fluid is saved in each interradius with the volume of $u_i(t)$ individually. The index i takes 1 to N anticlockwise; $N = 5$ in the case of five interradii. The total volume of fluid $\sum_{i=1}^{N} u_i(t)$ is constant in this situation, given that the mouth and genital slits closed during pumping. The pressure at each interradius is denoted by $p_i(t)$. Because it is difficult to experimentally determine the fluid property in the connection between the interradii, theoretical approaches to the fluid dynamics would be formidable attempts. However, with a rough estimation, the fluid would flow in a similar manner to Hagen-Poiseuille flow[10]. Accordingly, we assumed that the flow rate between the interradii is proportional to the pressure gradient; the time evolution of $u_i(t)$ is described as

$$\frac{\mathrm{d}u_i}{\mathrm{d}t} = \sum_{j=1}^{N} C_{ij}(p_j - p_i) \tag{1}$$

C_{ij} represents the ease with which fluid flows between the i-th and j-th interradii. It would be greater when the internal opening between the interradii is shorter and wider. We assumed that the value of C_{ij} for the nearest neighbors is larger than that for the others, based on the geometric distance as well as the observation that expansion in an interradius seemed to transfer mostly into a neighboring one (Supplementary Video S1).

The pressure $p_i(t)$ is given by the sum of the pressure generated by elastic membrane surrounding the interadius $p_{\mathrm{elas},i}(t)$, and the pressure actively generated by muscles $p_{\mathrm{mus},i}(t)$, namely,

$$p_i = p_{\mathrm{elas},i} + p_{\mathrm{mus},i} \tag{2}$$

We supposed that $p_{\mathrm{elas},i}(t)$ increases as the volume of fluid increases, and it is thus given by

$$p_{\mathrm{elas},i} = a u_i^m \tag{3}$$

where a represents the stiffness of the membrane. Considering that pumping makes a minute change in volume in a small size, $m = 1$ for simplicity. Meanwhile, we assumed that $p_{\mathrm{mus},i}(t)$ is given by

$$\tau \frac{\mathrm{d}p_{\mathrm{mus},i}}{\mathrm{d}t} = \overline{p}_{\mathrm{mus},i} - p_{\mathrm{mus},i} \tag{4}$$

where τ denotes the time constant. The target pressure $\overline{p}_{\mathrm{mus},i}$ is described as

$$\overline{p}_{\mathrm{mus},i} = \begin{cases} p_0 \text{ (shrinking period)} \\ 0 \text{ (expanding period)} \end{cases} \tag{5}$$

where p_0 is a positive constant. The expanding period switches to the shrinking period when u_i exceeds $u_{\max}$, while the shrinking period switches to the expanding period when u_i falls below $u_{\min}$.

At the beginning of the pumping phase, an interradius starts to shrink casually. On the assumption that a food largely occupies the interradius, we took the initial condition that one of the interradius has a larger volume than the others and is in the shrinking period, while the others are in the expanding period: $(u_1,\ p_1) = (u_{\mathrm{high}},\ a u_{\mathrm{high}}^m + p_0)$ and $(u_i,\ p_i) = (u_{\mathrm{low}} + \epsilon\xi_i,\ a(u_{\mathrm{low}} + \epsilon\xi_i)^m)$ for $i = 2, N$. Here, $u_{\mathrm{high}} > u_{\mathrm{low}}$, ϵ is a positive constant, and ξ_i takes a random value within $[-1.0, 1.0]$.

Simulation results showed that the interadii regularly moved in the unsynchronized sequence of 1-3-5-2-4 with suitably chosen parameters (Fig. 2a). The 1-4-2-5-3 pattern was also observed depending on the noise ξ_i. Our numerical simulations thus supported the experimental results well.

We focused on the fact that brittle stars sometimes have individual difference in the number of arms, namely, the number of interradii. Although five-armed animals are most common, there are six-armed animals in some cases. Simply changing the number of interradii from five to six led to a different synchronization pattern in the model simulation (Fig. 2b). Numbered from 1 to 6, the interradii moved in the synchronized sequence of 1, 3 and 5 together and then 2, 4 and 6 together repetitively; synchronized cycles in three distant ones followed that in the other three.

After $t = 4$, we assumed muscle fatigue to decrease p_0 gradually to zero, given the observation that the disk becomes relaxed at the end of the pumping phase. In both the case of $N = 5$ and 6, the cycles become longer and finally the oscillation vanishes in the same way as in the experiments (Fig. 2).

Behavior in a six-armed brittle star. We then obtained a six-armed individual with six symmetric interradii, in which pumping was also recognized. The interval between pumping phases was 19 ± 2 min (N = 1) after feeding (Fig. 3a). Each of the pumping phases continued for 39 ± 14 s (N = 1, n = 3) with the six interradii each repeating 2–4 cycles. The duration of shrinking and expanding periods at the beginning of the pumping phase was 5.4 ± 0.8 and 6.7 ± 0.6 s respectively, which became 5.7 ± 0.8 and 8.6 ± 1.6 s, respectively, at the end. The movements in the interradii were synchronized as occurs in the simulation (Fig. 3b, Supplementary Video S2).

Discussion

Based on the observation of pumping in the five-armed individuals of the green brittle star (Fig. 1b, Supplementary Video S1), we built a phenomenological model where a non-neuronal interaction robustly generated the rhythmic movement in five interradii (Fig. 2a), which is also applicable to the case of six interradii (Figs 2b, 3b, Supplementary Video S2). The correspondence to the real phenomena in the two morphological patterns suggests that the modelled interaction is likely to coordinate the animal's movement, independent of neuronal interactions between the interradii.

The difference in synchrony between five- and six-armed bodies can be explained by the volume and pressure. For the case of $N = 5$, the 1st interradius initially pushes its fluid into the 2nd and 5th ones, and then the 2nd and 5th push it into the 3rd and 4th, respectively. At the beginning, the difference between u_3 and u_4 is small. However, for example, when u_3 exceeds the upper threshold ($u_{\max}$) and u_4 is still in the expanding period, the fluid flows from the shrinking 3rd to the expanding 4th. The difference between u_3 and u_4 increases rapidly (by $t = 2$ in Fig. 2), so that each interradius in five-armed individuals makes an asymmetric flow into either neighbor. The direction of the rotation—1-3-5-2-4 or 1-4-2-5-3—depends on the initial perturbation, which is realized by the noise ξ_i in the model. In the absence of the noise, the pair 2nd–5th and the pair 3rd–4th each synchronized in simulation. For the case of $N = 6$, the fluid flows starting from the 1st interradius are propagated anticlockwise (1-2-3-4) and clockwise (1-6-5-4) and collide with each other at the 4th one. After the collision, the 4th pushes the fluid back to the 3rd and 5th. If the 3rd has a larger volume than the 5th, the pressure of the 3rd is also larger than that of the 5th based on the Eq. (3) because both are in the expanding period. Then following the Eq. (1), more fluid flows into the 5th than into the 3rd. As a result, u_3 and u_5 come to synchronize; the 4th acts as a buffer to eliminate the difference between u_3 and u_5. This mechanism causes each interradius in six-armed individuals to make symmetric flows into both neighbors, dividing the interradii into two synchronized groups.

Suppose pumping functions in a digestive process, this difference in coordination can be referred to intestinal movements. The interradii of five-armed individuals can make a travelling wave, which resembles peristaltic motion for transporting liquid matter in intestine[11]. On the other hand, the six-armed interradii can bring a stationary wave as recognized in segmental motion for mixing solid matter[11]. Accordingly, this individual difference in the brittle star could cause even a functional difference. Such difference in function might be a reason why the majority of extant brittle stars show pentaradial symmetry, not hexaradial symmetry. Investigation into

the function of pumping and comparative analyses of the efficiency between five- and six-armed bodies would provide more concrete understanding.

Previous studies explaining rhythmic movements in animals have built mathematical models assuming the existence of autonomous oscillatory activity of pacemaker neurons, so-called central pattern generators (CPGs)[1,12–15]. Robotics studies focusing on physical properties have also employed the idea of CPGs, as designed in each limb for locomotion[3,4] and in intestinal wall for peristalsis[16]. Even apart from animals, protoplasmic movement in the true slime mold has inspired physicists and robotics researchers to build mathematical models related to the number of circularly arranged oscillators[17,18]. Although this unicellular organism has no nervous system, these models have instead assumed spatially distributed biochemical oscillators in the body, which are similar to CPGs in concept. In this perspective, our model without explicit CPGs helps us begin to understand how biological movements take advantage of morphology, independent of spontaneous oscillation in neurons or biochemicals.

Although each pumping phase can be initiated singly by a non-neuronal interaction in the model, a series of pumping phases periodically occurred in the long run (Figs 1a, 3a). It could be supposed that long-term cycles of some matter such as neurotransmitters contribute to the initiation of pumping phases. The balance of neuronal and non-neuronal interactions in realizing the whole phenomenon of pumping should be investigated in further studies.

Methods

Intact adult individuals of the green brittle star *Ophiarachna incrassata* (Lamarck, 1816) were used in this study. They were obtained commercially and reared in laboratory aquariums (600 mm × 600 mm × 600 mm) filled with artificial seawater at 25–28 °C (TetraMarin Salt Pro, Tetra Japan Co, Tokyo, Japan; salinity, 32–35‰). The disks ranged 2–5 cm in diameter and mostly had five symmetric arms. We also obtained an individual that had six arms with a 4 cm diameter disk.

All animals were fed with dried krill (Tetra Krill-E, Tetra Japan Co, Tokyo, Japan). Once they detect the food, their arms capture it and carry it to their mouths. After a while, their disks start moving rhythmically. The long-term behavior of four randomly selected five-armed individuals and one six-armed animal were recorded using a time-lapse camera (TCL200, Brinno, Taipei, Taiwan). The short-term rhythmic movements of two randomly selected five-armed animals and the one six-armed animal were recorded three times for each from the aboral side with a video camera (EOS8000D, Canon, Tokyo, Japan) in small acrylic cases. Successfully recorded movements were analyzed using a video tracking software Kinovea (v. 0.8.15, http://www.kinovea.org/) at 10 f.p.s.

The numerical simulations of the mathematical model were carried out for $a = 1$, $p_0 = 20$, $u_{\max} = 0.5$, $u_{\min} = 0.1$, $\tau = 0.2$, $C_{ij} = 0.2$ for nearest neighbors, $C_{ij} = 0.02$ for the others. For the initial condition, $u_{\text{high}} = 1$, $u_{\text{low}} = 0.2$, and $\epsilon = 0.05$. After $t = 4$, p_0 is decreased constantly so that it becomes zero at $t = 6$.

Data Availability

The datasets generated during and/or analyzed during the current study are available from the corresponding author on reasonable request.

References

1. Grillner, S. Biological pattern generation: the cellular and computational logic of networks in motion. *Neuron* **52**, 751–766 (2006).
2. Talpalar, A. E. *et al*. Dual-mode operation of neuronal networks involved in left–right alternation. *Nature* **500**, 85 (2013).
3. Owaki, D., Kano, T., Nagasawa, K., Tero, A. & Ishiguro, A. Simple robot suggests physical interlimb communication is essential for quadruped walking. *J. R. Soc. Interface* **10**, 20120669 (2013).
4. Owaki, D. & Ishiguro, A. A quadruped robot exhibiting spontaneous gait transitions from walking to trotting to galloping. *Sci. Rep.* **7**, 277 (2017).
5. Kano, T. *et al*. A brittle star-like robot capable of immediately adapting to unexpected physical damage. *Roy. Soc. Open Sci.* **4**, 171200 (2017).
6. Kling, U. & Székely, G. Simulation of rhythmic nervous activities. *Kybernetik* **5**, 89–103 (1968).
7. Suzuki, R., Katsuno, I. & Matano, K. Dynamics of "neuron ring". *Kybernetik* **8**, 39–45 (1971).
8. Matsuoka, K. Sustained oscillations generated by mutually inhibiting neurons with adaptation. *Biol. Cybern.* **52**, 367–376 (1985).
9. Cobb, J. L. S. & Stubbs, T. R. The giant neurone system in Ophiuroids III: the detailed connections of the circumoral nerve ring. *Cell Tissue Res.* **226**, 675–687 (1982).
10. Sutera, S. P. & Skalak, R. The history of Poiseuille's law. *Ann. Rev. Fluid Mech.* **25**, 1–20 (1993).
11. Umetani, Y. & Inou, N. Biomechanical study of peristalsis: neural mechanism of rhythmic segmentation. *J. Soc. Inst. Contr. Eng.* **21**, 965–969 (1985).
12. Stein, P. S. Motor systems, with specific reference to the control of locomotion. *Ann. Rev. Neurosci.* **1**, 61–81 (1978).
13. Delcomyn, F. Neural basis of rhythmic behavior in animals. *Science* **210**, 492–498 (1980).
14. Grillner, S., McClellan, A. & Perret, C. Entrainment of the spinal pattern generators for swimming by mechano-sensitive elements in the lamprey spinal cord *in vitro*. *Brain Res.* **217**, 380–386 (1981).
15. Marder, E. & Calabrese, R. L. Principles of rhythmic motor pattern generation. *Physiol. Rev.* **76**, 687–717 (1996).
16. Kano, T., Kawakatsu, T. & Ishiguro, A. Generating situation-dependent behavior: decentralized control of multi-functional intestine-like robot that can transport and mix contents. *J. Robot. Mech.* **25**, 871–876 (2013).
17. Takamatsu, A. *et al*. Spatiotemporal symmetry in rings of coupled biological oscillators of *Physarum* plasmodial slime mold. *Phys. Rev. Lett.* **87**, 078102 (2001).
18. Umedachi, T., Idei, R., Ito, K. & Ishiguro, A. A fluid-filled soft robot that exhibits spontaneous switching among versatile spatiotemporal oscillatory patterns inspired by the true slime mold. *Artif. Life* **19**, 67–78 (2013).

Acknowledgements

We thank Prof. Philip L. Newland for his critical comment upon our manuscript. We are grateful to Prof. Takeshi Kano for deeply discussing our mathematical model. This work was partly supported by JSPS KAKENHI (Grant Number 16KT0099) and by JST CREST (Grant Number JPMJCR14D5), Japan.

Author Contributions

D.W., Y.H. and H.A. observed and analyzed the rhythmic movement. D.W., Y.H. and H.A. built the mathematical model. D.W., Y.H. and H.A. wrote the manuscript.

Additional Information

Supplementary information accompanies this paper at https://doi.org/10.1038/s41598-019-44808-w.

Competing Interests: The authors declare no competing interests.

Publisher's note: Springer Nature remains neutral with regard to jurisdictional claims in published maps and institutional affiliations.